Environmental Science
Water Research & Technology

Accepted Manuscript

This article can be cited before page numbers have been issued, to do this please use: J. Deaver, T. Solon, A. Grunden and D. F. Call, *Environ. Sci.: Water Res. Technol.*, 2026, DOI: 10.1039/D5EW01105A.

View Article Online
DOI: 10.1039/D5EW01105A

Water Impact Statement

Unstable biological phosphorus removal remains an ongoing challenge for many water resource recovery facilities (WRRFs). Improving the stability of the biological process can increase WRRF confidence in the process. We find strong evidence that unstable phosphorus removal at a full-scale WRRF is associated with significant changes in the activity of abundant polyphosphate accumulating organisms, likely driven by changes in redox conditions across the biological basins.

View Article Online
DOI: 10.1039/D5EW01105A

Disruption in Gene Expression Cycles of Polyphosphate Accumulating Organisms is Associated with a Full-Scale Enhanced Biological Phosphorus Removal Instability Event

Jessica A. Deaver[1,2], Thomas Solon[3,4], Amy M. Grunden[2,5], and Douglas F. Call[1,2,*]

[1]Department of Civil, Construction, and Environmental Engineering, North Carolina State University, Raleigh, NC 27606

[2]Science and Technologies for Phosphorus Sustainability (STEPS) Center, North Carolina State University, Raleigh, NC 27606

[3]Department of Environmental Engineering and Earth Sciences, Clemson University, SC 29634

[4]Renewable Water Resources (ReWa), Greenville, SC 29607

[5]Department of Plant and Microbial Biology, North Carolina State University, Raleigh, NC 27606

*corresponding author, dfcall@ncsu.edu

Abstract

Enhanced biological phosphorus removal (EBPR) enriches polyphosphate accumulating organisms (PAOs) via alternating anaerobic/aerobic feast-famine cycles to remove phosphorus from wastewater. EBPR can be prone to instability though the causes are often unclear. Genome-centric metatranscriptomics was used to investigate EBPR instability event at a full-scale facility that typically experiences a winter instability event to identify changes in microbial community composition and gene expression

View Article Online
DOI: 10.1039/D5EW01105A

characteristic of reduced EBPR performance. The facility sampled operates an Anaerobic/Anoxic/Aerobic (A2O) EBPR process. Notably, process monitoring data indicated few process changes beyond increased effluent phosphorus (> 3 mg/L compared to typical concentrations < 0.5 mg/L) and lower water temperatures during the instability event. Microbial community composition remained consistent before, during, and after the instability event. Two PAO MAGs, *Ca. Accumulibacter phosphatis* and *Ca. Accumulibacter propinquus*, were the most abundant and transcriptionally active PAOs. DESeq2 analyses of significantly (adjusted p-value < 0.01) and differentially ($|\log_2(\text{FoldChange})| > 1$) expressed genes revealed that expression of key carbon metabolism, energy metabolism, and denitrification genes that typically peak in the anaerobic zone under anaerobic, high carbon conditions shifted to peak in the anoxic zone during the instability. These results demonstrate a shift in PAO activity, and not community composition, associated with a full-scale EBPR instability event.

Introduction

Water resource recovery facilities (WRRFs) often remove phosphorus from wastewater via enhanced biological phosphorus removal (EBPR). In EBPR alternating anaerobic and aerobic zones enrich polyphosphate accumulating organisms (PAOs). PAOs uptake soluble carbon, such as volatile fatty acids (VFAs) and sugars, and store it intracellularly, in forms such as polyhydroxyalkanoates (PHAs), under anaerobic conditions. PAOs generate the energy (i.e., ATP) and reducing power (e.g., NADH) to internally store carbon by degrading stores of glycogen and polyphosphate (poly-P). Then, under aerobic conditions, PAOs respire on oxygen gas and oxidize internal carbon

View Article Online
DOI: 10.1039/D5EW01105A

for growth and cell division, replenishing their stores of glycogen and poly-P and removing phosphorus from the bulk solution in the process.

Phosphorus removal in full-scale EBPR can become unstable, often for reasons not well understood.[1] Many factors may contribute to EBPR stability, or lack thereof, including the redox conditions and the concentration of VFAs entering the anaerobic stage.[2,3] Side stream EBPR (S2EBPR) can help with stability by improving VFA supply and enabling a sufficiently reduced redox environment.[4] Some process data and EBPR stability correlate, including positive relationships between readily biodegradable chemical oxygen demand (rbCOD) to influent phosphorus ratios and effluent total phosphorus (TP). Other process data such as biochemical oxygen demand (BOD):TP and COD:TP are often not directly correlated.[3] Consequently, deciphering the root cause of full-scale EBPR instabilities from process data is challenging. Deeper insight into the underlying biology may help reveal causes of instability.

Our knowledge of the microorganisms involved and the biochemical pathways they use is primarily limited to stable EBPR. Full-scale EBPR systems that experience instabilities have received less attention. The most dominant PAOs in stable EBPR systems globally belong to the genera *Candidatus (Ca.) Accumulibacter*, *Azonexus* (formerly *Dechloromonas*), and *Ca. Phosphoribacter* (formerly *Tetrasphaera*).[5] *Ca. Accumulibacter* are considered the canonical model for PAO metabolism, though it is now known that there can be vast diversity between different *Ca. Accumulibacter* strains.[6,7] In unstable systems, linkages between microbial community and activity dynamics and instability are limited.[8–10] Lindner et al.[10] used genome-centric metagenomics and metatranscriptomics on two samples collected during stable operation and two samples

View Article Online
DOI: 10.1039/D5EW01105A

collected approximately six weeks later during unstable operation. They observed unstable P removal associated with changes in mixed liquor suspended solids, decreased VFA loads, and increased primary effluent orthophosphate, and they reported genus level changes in *Ca. Accumulibacter* relative abundance and carbon metabolism gene expression during unstable EBPR. However, low sample numbers and the length of time between sampling events makes it difficult to discern if the shift in community dynamics led to the instability or vice versa.

In this study, we utilized metagenome-based transcriptomics to investigate changes, or lack thereof, to microbial community structure and regulation of population-specific pathways before versus during an instability event occurring within two solids retention times (SRTs) at a full-scale WRRF with an anaerobic/anoxic/oxic (A2O) process configuration. This facility historically experiences EBPR instability in the winter, so we conducted our sampling campaign during that time. We collected samples throughout two parallel treatment trains on three days before, during, and after an instability event defined by effluent phosphorus exceeding 1 mg-P/L. We used metagenomic *de novo* assemblies and phylogenomic comparisons to conduct a species-level identification of key PAOs, and mapped RNA reads to metagenome-assembled genomes (MAGs) to identify expression-level gene changes. Our findings show that shifts in PAO activity, and not community composition, can be associated with a full-scale instability event.

View Article Online
DOI: 10.1039/D5EW01105A

Material and Methods

Facility Description. The WRRF studied (operated by Renewable Water Resources in Greenville, SC, USA) is in the southeastern United States. During the study period, it treated an average daily flow of 16 million gallons per day (MGD) of primarily residential and industrial wastewater from a combined sewer system. The facility performs biological nitrogen and phosphorus removal via three parallel A2O treatment trains that each receive an equal proportion of primary clarifier effluent. The SRT of the A2O process during the study was ~10 days with a mixed liquor return rate of 6.4 MGD. The anaerobic mass fraction was ~13.5%, which was calculated with the following equation, where F_{ANA} is fraction of mass in the anaerobic zone.

$$F_{ANA} = \frac{Mass\ of\ sludge\ in\ the\ anaerobic\ zone}{Total\ mass\ of\ sludge}\ x\ 100\%$$

The facility typically adds waste from a juice processing facility as a supplemental carbon source. Influent measurements were taken at a pump station composite sampler that includes side stream flow back to the head of the plant (~1 MGD). Effluent measurements were collected post deep bed sand filters, UV disinfection, and re-aeration using a composite sampler. The facility historically experiences unstable EBPR in the winter (**Figure S1**), which guided decisions on when to collect more comprehensive sets of samples (i.e., samples for DNA/RNA sequencing across all redox zones and two parallel basins).

Sample collection. Fresh activated sludge (AS) samples were collected and preserved for DNA and/or RNA sequencing. Approximately 500-mL of AS was collected at multiple sampling locations along two A2O basins (**Figure 1**) and sub-sampled as described in

View Article Online
DOI: 10.1039/D5EW01105A

Supplementary Information. Samples preserved in 2x DNA/RNA Shield solution (Zymo Research, Irvine, CA, USA) were shipped at room temperature to NC State University (Raleigh, NC, USA), where they were aliquoted into 2-mL tubes and stored at −20°C until further processing. To collect samples for simultaneous orthophosphate measurements, an 8 mL subsample was immediately filtered with a 0.45 µm filter and shipped overnight on ice to NC State.

DNA sequencing using both short read (Illumina) and long read (Oxford Nanopore) technology was performed on eight samples collected from the end of the aerobic zone (location G in **Figure 1**) of two parallel treatment trains on 11/20/2023, 11/29/2023 (unstable EBPR), 12/6/2023, and 2/23/2024 (**Table S1**). RNA sequencing using short read (Illumina) technology was performed on 30 samples collected from the beginning and end of each zone (locations A through G in **Figure 1**) of two parallel treatment trains on 11/20/2023 (n=12), 11/29/2023 (n=6), and 12/6/2023 (n=12). The samples collected from the same location in each of the two parallel treatment trains were considered biological replicates (n=2 per sample location per date). On 11/29/2023 samples were only collected from the end of each redox zone (Locations B, D, and G) due to time constraints. Samples for RNA sequencing were collected on 2/23/2024 (n=6) as well, however, the facility was experiencing reduced nitrification at that time, so it was decided to exclude those samples from further metatranscriptomic analyses but include them in the metagenomic draft genome reconstruction.

Sample processing and nucleic acid extractions. DNA was extracted using the FastDNA Spin Kit (MP Biomedicals, Santa Ana, CA, USA) with modifications described in

View Article Online
DOI: 10.1039/D5EW01105A

Supplementary Information. DNA was eluted in 50 µL of 10 mM Tris-HCl at pH 8.0 and stored in multiple aliquots at −20°C.

RNA was extracted using the ZymoBiomics RNA miniprep kit (Zymo Research) following the manufacturer's protocols with modifications described in Supplementary Information. RNA was stored in multiple aliquots at −80°C.

DNA and RNA purity was assessed using a Nanodrop Spectrophotometer ND-1000 (ThermoFisher Scientific, Waltham, MA, USA), and quantity was assessed using dsDNA BR assays and RNA BR assays with a Qubit 3.0 Fluorometer (ThermoFisher Scientific). DNA and RNA integrity were evaluated using gDNA and RNA ScreenTape Analyses on an Agilent 4150 TapeStation (Agilent Technologies, Inc., Santa Clara, CA, USA).

Library preparation and sequencing. For Oxford Nanopore sequencing, DNA libraries were prepared using the Native Barcoding Kit 24 V14, SQK-NBD114, according to the manufacturer's protocols (Oxford Nanopore Technologies, Oxford, UK). Samples were pooled at equimolar concentrations and run on an Oxford Nanopore MinION Mk1C device with a R14 FLO-MIN114 flow cell. The flow cell was run within one month of delivery and run for 48 hours. The data output equaled 16.5 Gbp with an estimated N50 of 7.2 kbp.

For Illumina sequencing, DNA and RNA samples were shipped frozen to Admera Health, LLC (South Plainfield, NJ, USA). DNA libraries were prepared using a KAPA HyperPrep kit (Roche, Indianapolis, IN, USA) according to the manufacturer's protocols and sequenced 2 x 150-bp on an NovaSeqX Plus 10B (Illumina, San Diego, CA, USA). One third of the RNA samples were treated with DNase due to evidence of DNA

View Article Online
DOI: 10.1039/D5EW01105A

contamination found during QC. Final RNA Integrity Numbers (RIN) were all > 7. All RNA samples were then rRNA depleted using a QIAseq FastSelect Epidemiology kit (for bacteria, human, mouse, and rat rRNA) (Qiagen, Hilden, Germany), and RNA libraries were prepared using a NEB Ultra II Directional RNA Library Prep kit (New England Biolabs, Ipswich, MA, USA). RNA was sequenced 2 x 150-bp on an NovaSeqX Plus 10B (Illumina). Total reads sequenced equaled approximately 70 million paired end reads per DNA or RNA sample. DNA and RNA sequencing reads are available in NCBI under BioProject PRJNA1232215.

Metagenomic assembly, binning, and annotation. Detailed information about assembly, binning, and genome annotation is described in Supplementary Information and example scripts used for analyses are provided at https://github.com/jadeaver/bioP_MAGs. Briefly, demultiplexed short reads received from Admera were quality checked with FastQC (v0.12.1).[12] Raw long read sequences were basecalled with Oxford Nanopore's basecaller Dorado using the super accurate model version 4.3.0 (https://github.com/nanoporetech/dorado), quality checked with Nanoplot (v1.42.0), and filtered using Filtlong (v0.2.1).[13] Long reads were polished with short reads using Ratatosk (v0.9.0) and assembled using Flye (v.2.9.4).[14,15] Each sample was individually assembled, samples collected on the same day were co-assembled, and all samples were co-assembled for a total of 13 assemblies (**Table S2**). Each assembly was binned using both maxbin2 (v2.2.7) and metabat2 (v2.15.2) accounting for differential coverage of all eight samples.[16,17] Bins derived from the same assembly were dereplicated with DasTool (v1.1.7)[18] and remaining bins were further dereplicated at a 95% average

View Article Online
DOI: 10.1039/D5EW01105A

nucleotide identity (ANI) threshold across all assemblies using dRep (v3.5.0) to select the best quality representatives at approximately the species-level.[19] Genomes were preliminarily classified using the GTDB-Tk classify workflow (v2.4.0), quality checked with CheckM (v1.1.6) and annotated with Bakta (v1.9.4) using the full Bakta database (v5.1).[20–22]

Phylogenomic analyses and relative abundance. Reference genomes from Petriglieri et al.[23] were downloaded using NCBI datasets and phylogenomic trees created with GToTree (v1.8.8) using the Proteobacteria HMM profiles.[24] More details are provided in Supplementary Information. FastANI (v1.34) was used to perform pairwise average nucleotide identity (ANI) comparisons between reference genomes and PAO MAGs assembled during this study to assign taxonomy.[25] Taxonomic profiles of individual metagenomes and MAG recovery were assessed with SingleM (v0.18.3).[26] The R package vegan was used to calculate β-diversity based on Bray-Curtis distances using the SingleM genus-level relative abundance table as input.[27] A subsequent PERMANOVA test performed on the calculated distances based on date (n=2 per date) and basin (n=3 per basin). Scripts used for these analyses are available at https://github.com/jadeaver/bioP_MAGs.

Metagenome-enabled transcriptomics. Detailed information about gene expression analyses is described in Supplementary Information and scripts used for analyses are provided at *https://github.com/jadeaver/bioP_MT*. Briefly, RNA reads were quality checked with FastQC, adapters removed using fastp (v0.23.4), and rRNA sequences

View Article Online
DOI: 10.1039/D5EW01105A

filtered out with SortMeRNA (v4.3.7) leaving 30-45 million paired end reads per sample remaining.[28,29] When possible, MAGs recovered from this study were used as references for transcript quantification. For *Ca. Accumulibacter* species identified as present in the metagenomes but not recovered during binning, species-level representative MAGs (as defined by Petriglieri et al.[23]) were used as references. The predicted coding regions were concatenated together to create a mapping index of *Ca. Accumulibacter* MAGs. Quality processed metatranscriptomic reads from all samples were competitively pseudoaligned to the mapping index and quantified with kallisto (v0.51.0).[30] DESeq2 was used for statistical analyses of differentially expressed genes.[31] Multiple contrasts were performed between groups defined as the zone and day (i.e., “Anaerobic 11/20/23”, “Anoxic 12/6/23”, etc.) and the results are reported here. As a note, multiple contrasts were performed between location groups defined as the exact sample location and day (i.e., “Location B 11/20/23”, “Location D 12/6/23”, etc.) to examine how considering precise location versus multiple sample locations within the same zone impact results. Results were consistent with each other, and therefore, we present the data from zone/day groups here.

Results and Discussion

Full-scale EBPR performance. The facility experienced a winter instability event during which peak effluent TP concentrations exceeded 3 mg-P/L (**Figure 2A**). Any measurement over 1 mg-P/L was considered unstable performance; thus, this event lasted ~7 days. **Table 1** summarizes facility performance during the study period. Notably, temperature decreased by approximately 3.4^{o}C from mid-November to mid-December.

View Article Online
DOI: 10.1039/D5EW01105A

Supplemental juice waste and acetic acid was added to support EBPR during this period. In response to the instability, alum was added after the final clarifiers and before the sand bed filters from 11/28/23 to 11/30/23, resulting in effluent TP concentrations returning to < 0.5 mg-P/L. Alum did not impact orthophosphate concentrations measured in the anaerobic, anoxic, and aerobic zones because it was not recycled back to the biological process. End of anaerobic zone orthophosphate concentrations averaged 25.1±10.6 mg-P/L from November 13 to December 15 (**Figure 2B**). Orthophosphate concentrations measured at the end of the anoxic zone for the same time averaged 8.1±2.6 mg-P/L and remained relatively consistent throughout the instability event. End of aerobic zone orthophosphate concentrations measured < 0.5 mg-P/L during stable operation and exceeded 1 mg-P/L, peaking around 3 mg-P/L, during instability.

MAG assembly and classification. In total, 53 MAGs were recovered after species-level dereplication at 95% ANI. Twenty-two were high-quality (HQ) per MIMAG standards with > 90% completion, < 5% redundancy, presence of the 23S, 16S, 5S rRNA genes, and > 18 tRNA genes (**Table S3**).[32] The remaining MAGs were medium quality (MQ) with > 75% completion, < 10% redundancy, and most included the presence of all rRNA genes and > 18 tRNA genes. Of these, six MAGs (two HQ and four MQ) were taxonomically classified as PAOs belonging to either *Ca. Accumulibacter* or *Azonexus* lineages according to GTDB-Tk classification.

To further classify the PAO MAGs, we performed phylogenomic analyses to compare the four *Ca. Accumulibacter* MAGs reported here to the species representatives defined by Petriglieri et al.[23] (**Figure S2A, Table S4**). *Ca. Accumulibacter* lineages have

View Article Online
DOI: 10.1039/D5EW01105A

been divided into 18 clades based on comparison of their *ppk1* genes. Genome-based comparisons accurately reflect *ppk1*-based phylogeny.[23,33] Pairwise ANI comparisons and phylogenomic tree construction based on Proteobacteria hidden Markov model (HMM) profiles indicated that MAG 010, MAG 12, and MAG 11 belong to the species *Ca. Accumulibacter phosphatis* (clade IIA), *Ca. Accumulibacter propinquus* (clade IIB), and *Ca. Accumulibacter conexus* (clade IIF), respectively. MAG 166 likely belongs to a new species cluster, *Ca. Accumulibacter* UW 21, proposed by Stewart et al.[33] The ANI value between MAG 166 and *Ca. Accumulibacter* UW 21 is 97.1%, suggesting that MAG 166 tracks to the same species as UW 21.

GTDB-based classifications indicated two MAGs, MAG 109 and MAG 311, belong to the *Azonexus* lineage. Pairwise ANI comparisons indicated neither *Azonexus* MAG belonged to either *Azonexus phosphoritrophus* or *Azonexus phosphorivorans*, the two *Azonexus* species whose contributions to EBPR have been best characterized.[34] Pairwise ANI comparisons to GTDB *Azonexus* representative MAGs ranged from 78% to 99% with MAG 109 most closely matching *Azonexus sp009469585.* (GCA_009469585.1) at 92% ANI and MAG 311 most closely matching *Azonexus sp020621865* (GCA_020621865.1) at 99% ANI (**Figure S2B**, **Table S5**). Further analyses are necessary to determine what role, if any, these *Azonexus* species play in phosphorus removal. Considering their low abundance and activity (described below), we did not further investigate these MAGs.

Community composition and transcriptional profiles. To estimate overall microbial community relative abundance and to ensure the most abundant PAOs were represented

View Article Online
DOI: 10.1039/D5EW01105A

by the recovered MAGs, we profiled the raw metagenomes with SingleM. Genus-level profiles demonstrated that *Ca. Accumulibacter* was the most abundant genus on all days with an average relative abundance of 6.8±0.2%, 5.8±0.1%, and 6.1±0.1% on 11/20/23, 11/29/23, and 12/6/23, respectively (**Figure 3A**). Approximately 25% of the community was not classified at the genus level (data not shown), and approximately 30% of the community was represented by a genus with a relative abundance of 1% or more. A diverse, highly redundant microbial community where few individuals dominate is typical of full-scale activated sludge communities. In this study, β-diversity was calculated based on Bray-Curtis distances. A subsequent PERMANOVA test performed on the calculated distances based on date (n=2 per date) and basin (n=3 per basin) groupings revealed that date had a greater effect than basin (R^2=0.829 for date versus R^2=0.171 for basins) but that overall genus-level community composition changes were not significant over the instability event (p-value = 0.067) (**Figure S3**). The community results suggest that unstable phosphorus removal was not caused by changes in genus-level microbial community structure.

To explore if changes in PAO population structure were linked to the instability, species-level profiles of *Ca. Accumulibacter*, *Azonexus*, and Ca. *Phosphoribacter* were further assessed from SingleM output. There were nine *Ca. Accumulibacter* and one *Azonexus* species each comprising more than 0.25% of the total community composition in at least one sample (**Figure 3B**). *Ca. Accumulibacter phosphatis* and *Ca. Accumulibacter propinquus* were identified in the highest proportions, comprising about 1/3 and 1/5 of the PAO community, respectively, across all sampling dates. *Ca. Accumulibacter contiguus*, *Ca. Accumulibacter cognatus*, *Ca. Accumulibacter vicinus*,

View Article Online
DOI: 10.1039/D5EW01105A

and *Ca. Accumulibacter necessarius* were identified in the raw metagenomes, but MAGs were not recovered.

The four *Ca. Accumulibacter* MAGs recovered in this study and the species representative MAGs [23] for *Ca. Accumulibacter contiguus*, *Ca. Accumulibacter cognatus*, *Ca. Accumulibacter vicinus*, and *Ca. Accumulibacter necessarius* were used as reference genomes for further metatranscriptomic analysis. Metatranscriptomic profiling of *Ca. Accumulibacter* species demonstrated that the most abundant *Ca. Accumulibacter* MAGs also contributed the most to the transcriptional profile of the *Ca. Accumulibacter* community with 44%-52% of RNA reads mapping to *Ca. Accumulibacter phosphatis* (MAG 010) or *Ca. Accumulibacter propinquus* (MAG 12) (**Figure 3C**). The lack of changes in composition or transcript profiles of the PAO populations indicated that a shift in who was present and active in the microbial community did not contribute to the instability event. The facility's SRT is 10 days, so if a shift did occur, we would expect it to be captured between the first and last samples collected 16 days apart. While this study suggests community composition changes did not contribute to the instability event, a study by Lindner et al.[10] demonstrated a microbial community shift in connection with an EBPR instability event. Microbial community composition shifts might occur in response to an instability, rather than being the cause of the instability itself. Further investigations into instability events at other facilities are necessary to confirm if microbial community composition is more likely to be a lagging indicator of instability, rather than a leading indicator.

View Article Online
DOI: 10.1039/D5EW01105A

Gene expression profiles across redox zones. We performed differential gene expression analyses on *Ca. Accumulibacter phosphatis* and *Ca. Accumulibacter propinquus*, the two PAOs with the highest relative abundance and greatest contribution to the PAO transcript profile. DESeq2 analyses between redox zones on 11/29/23 (unstable EBPR) and 12/6/23 suggested most genes were differentially expressed in the anoxic zone between 11/29/23 (unstable EBPR) and 11/20/23 (**Figure S4**). To further explore this phenomenon, we used DESeq2 to compare the number of differentially (log_2[FoldChange] > 1 or < -1) and significantly (adjusted p-value < 0.01) expressed genes across redox zones on each sampling day. For *Ca. Accumulibacter phosphatis*, before the instability, there were 80 significantly (adjusted p-value < 0.01) differentially expressed genes with a log_2(FoldChange) > 1 or < -1 between the anaerobic and aerobic zones, 38 between the anaerobic and anoxic zone, and only one between the anoxic and aerobic zone (**Table 2**, **Figure 4**). During the instability event, the reverse was true. There were 68 significantly differentially expressed genes with a log_2[FoldChange] > 1 or < -1 between the anoxic and aerobic zone, but only 11 between the anaerobic and anoxic zone and 1 between the anaerobic and aerobic zone. *Ca. Accumulibacter propinquus* also exhibited the same gene expression patterns (**Figure S5).**

Many genes differentially expressed between the anaerobic and aerobic zones on days 11/20/23 and 12/6/23 were the same genes differentially expressed between the anoxic and aerobic zones on day 11/29/23 (unstable EBPR) (**Figure 5A**). Cyclical gene expression has been identified in studies of *Ca. Accumulibacter*-enriched SBRs, and we found that many of the genes whose expression patterns changed during the instability event deviated from typical patterns identified in lab-scale studies and observed during

View Article Online
DOI: 10.1039/D5EW01105A

stable phosphorus removal. For example, Oyserman et al.[35], performed metatranscriptomic analyses on a SBR enriched in *Ca. Accumulibacter* operating under alternating anaerobic/aerobic, feast/famine conditions and identified various expression trends (e.g., upregulation during the redox transition) of genes involved in carbon metabolism, denitrification, and energy production. Genes involved in those same metabolic pathways exhibited cyclical gene expression patterns in this study, however, when those genes were expressed shifted during the instability. Genes exhibited peak expression in the anoxic zone, rather than the anaerobic zone, during the instability (**Figure 5B)**.

Genes exhibiting a shifted expression pattern included several *Ca. Accumulibacter phosphatis* carbon metabolism genes. These genes were differentially expressed in samples obtained from the anaerobic zone (compared to the aerobic zone) on days 11/20/23 and 12/6/23. Those same genes were differentially expressed in the anoxic zone (compared to the aerobic zone), rather than the anaerobic zone, on day 11/29/23 (unstable EBPR). These genes included PHA synthesis related genes such as *phaC* and *phaR* and methylmalonyl mutase genes. For example, the gene *phaC* was differentially expressed between the anaerobic and aerobic zones on 11/20/23 ($\log_2$[FoldChange] = 1.3, adjusted p-value = 2 x 10^{-5}). However on 11/29/23 (unstable EBPR) it was not significantly differentially expressed between the anaerobic and aerobic zone, but rather between the anoxic and aerobic zone ($\log_2$[FoldChange] = 2.1, adjusted p-value = 7.6 x 10^{-7}) (**Figure 5**).The *phaC* gene encodes a subunit of PHA synthase, and its anaerobic expression is considered a hallmark feature of *Ca. Accumulibacter* during phosphorus release.[6,35,36] In Oyserman et al.[35] PHA synthesis genes *phaC* and *phaR* exhibited

View Article Online
DOI: 10.1039/D5EW01105A

upregulation under high acetate, anaerobic conditions. The genes for methylmalonyl mutase and its associated GTPase also exhibited peak expression in the anoxic zone rather than the anaerobic zone on 11/29/23 (unstable EBPR) exhibiting $\log_2$[FoldChange] = 0.97 (adjusted p-value = 0.004) and 1.1 (adjusted p-values = 0.003), respectively. Methylmalonyl mutase and its associated GTPase are involved in the conversion of succinyl-CoA to methylmalonyl-CoA in the split mode TCA cycle utilizing the methylmalonyl-CoA pathway. Various metabolic models exist to explain how *Ca. Accumulibacter* consumes and stores carbon while balancing energy and reducing equivalents, including the full TCA cycle, the split mode TCA cycle, and the glyoxylate shunt models. It is likely that *Ca. Accumulibacter* possess metabolic flexibility that enables them to thrive in dynamic conditions.[7] *Ca. Accumulibacter* are suggested to use the methylmalonyl-CoA pathway in particular during anaerobic PHA synthesis from mixed carbon sources, including co-utilization of glutamate and acetate, aspartate, lactate, and succinate.[37,38] Chen et al.[38] noted greater anaerobic methylmalonyl-CoA mutase gene expression in variable carbon source, anaerobic/aerobic batch tests performed on SBR enrichment cultures suggesting its involvement in anaerobic PHA synthesis particularly under mixed carbon feed conditions. We cannot determine the actual pathways used by the *Ca. Accumulibacter phosphatis* populations in this study, but expression of TCA cycle, glyoxylate shunt, and methylmalonyl-CoA pathway genes demonstrated capabilities for a dynamic response. The shift in expression dynamics of key carbon metabolism genes suggests that a disruption to carbon cycling under stable phosphorus removal occurred during the instability event.

View Article Online
DOI: 10.1039/D5EW01105A

Denitrification gene expression also changed during the instability event. *Ca. Accumulibacter phosphatis* (MAG 010) possessed genes encoding enzymes in every step of denitrification (**Figure 6**). Denitrification potential has been reported for other *Ca. Accumulibacter phosphatis* MAGs.[39] Both sets of nitrate reductase genes, *napAB* and *narGH* were annotated in the *Ca. Accumulibacter phosphatis* MAG recovered in this study. In addition, *norB*, encoding the nitric oxide large subunit, was annotated. The gene encoding the nitric oxide small subunit, *norC,* was not annotated, however, possibly due to gaps in assembly or annotation of the MAG. All annotated genes encoding denitrification enzymes, except for *nirS*, encoding nitrite reductase, were significantly upregulated in the anoxic zone compared to the aerobic zone on 11/29/23 (unstable EBPR) ($\log_2$[FoldChange] > 1.5, adjusted p-value $\leq$ 0.004) (**Figure 5A**). These genes exhibited a shift in expression where peak expression (in TPM) occurred in the anoxic zone instead of the anaerobic zone on 11/29/23 (**Figure S6)**. *nirS* gene expression stayed consistent between the anaerobic and anoxic zone on 11/29/23 rather than peaking in the anaerobic zone even though it was not identified as significantly differentially expressed by DESeq2 analysis. Previous studies exploring *Ca. Accumulibacter* gene expression cycles between anaerobic/aerobic, feast/famine cycles have noted an increase in expression of denitrification genes after anaerobiosis.[39,40] Stable EBPR on 11/20/23 was characterized by the same expression pattern, with denitrification gene expression peaking in the anaerobic zone samples, and a return to this expression pattern is noted on 12/6/23.

Energy metabolism genes important to denitrification also exhibited shifted gene expression cycles. Genes including several encoding respiratory chain components such

View Article Online
DOI: 10.1039/D5EW01105A

as cytochrome b, cytochrome c proteins, cytochrome c biogenesis proteins, F0F1 ATP synthase genes, and electron transfer flavoproteins were significantly upregulated in the anoxic zone (vs. the aerobic zone) rather than the anaerobic zone (vs. the aerobic zone) on 11/29/23 (unstable EBPR) (adjusted p-value < 0.01, log2[FoldChange] > 1) (**Figure 5A**). For example, the gene for the F0F1 ATP synthase B subunit was differentially expressed between the anaerobic and aerobic zones on 11/20/23 (log_2[FoldChange] = 1.2, adjusted p-value = 6.1 x 10^{-8}) and differentially expressed between the anoxic and aerobic zone on 11/29/23 (unstable EBPR) (log_2[FoldChange] = 1.6, adjusted p-value = 6.1 x 10^{-7}). Aerobic respiration and denitrification depend on the same core respiratory machinery and are thought to have co-evolved.[41] Shared machinery includes NADH dehydrogenase (complex I), the cytochrome bc1 complex (complex III), and cytochrome c. The F0F1 ATP synthase genes encode the machinery for generating ATP from the proton motive force generated by the respiratory chain enabling energy yield from either final electron acceptor.[42] For PAOs, pit transport of inorganic phosphate hydrolyzed from poly-P is thought to be the primary mode of proton motive force production that in turn drives carbon uptake (e.g., acetate via the ActP transporter) and ATP production via F0F1 ATP synthase.[43] Previous studies suggest that clade IIA *Ca. Accumulibacter* cannot respire on nitrate despite possessing a *nap* operon.[40,44] Presence and expression of *narGH* in addition to *napAB* suggest that nitrate respiration may be possible. The delayed upregulation of key denitrification and associated energy production genes suggests a disruption of typical energy metabolism activity occurred during the instability event.

Ca. Accumulibacter propinquus (MAG 12) exhibited the same shifts in gene expression patterns of similar denitrification and energy metabolism associated genes

View Article Online
DOI: 10.1039/D5EW01105A

(**Figure S7**). Nitrate reductase gene *napA* was the only denitrification gene that exhibited a shift in significant differential gene expression (adjusted p-value < 0.01, $\log_2$[Foldchange] > 1). *Ca. Accumulibacter propinquus* did not contain annotations for nitric oxide reductase (*norBC*) and nitrous oxide reductase (*nosZ*) genes. Associated respiratory machinery genes exhibited the shift to anoxic upregulation, including cytochrome c, cbb3-type cytochrome c oxidase subunit I, and two F0F1 ATP synthase subunits. The cbb3-type cytochrome c oxidase subunit I is of note because its high substrate affinity and tendency to be expressed under microaerobic conditions.[45] Camejo et al.[40] identified a full denitrification pathway in a clade IC *Ca. Accumulibacter* MAG (UW-LDO-IC) enriched in an anaerobic/microaerobic SBR. UW-LDO-IC gene expression patterns also suggested coregulation of denitrification and high oxygen affinity cbb3-type cytochrome genes with expression peaking at the anaerobic/microaerobic transition. Delayed expression of *Ca. Accumulibacter propinquus* genes typically expressed following anaerobic contact further demonstrate that PAO activity changes characterize the instability event.

Implications for full-scale EBPR stability. Our findings indicate that unstable phosphorus removal at the full-scale facility in this study was associated with changes in “what” the PAOs were doing rather than “who” was present. This finding is different from that described by Lindner et al.[10], wherein they found changes in PAO relative abundance between stable and unstable operation in addition to changes in carbon metabolism gene expression. The major changes we observed were shifts in pathways associated with carbon utilization, denitrification, and energy metabolism across the redox zones. As a

View Article Online
DOI: 10.1039/D5EW01105A

result, aerobic uptake of phosphorus was delayed and phosphorus concentrations leaving the aerobic zone were elevated compared to stable conditions.

The shifted pathways illustrated in **Figure 6** are largely involved in carbon metabolism, denitrification, and bioenergetics, key metabolic pathways with implications for poly-P accumulation. Though we cannot definitively say what caused the changes in PAO activity, we hypothesize based on our results that either the redox conditions of the anaerobic zone conditions and/or influent VFA composition contributed. The shift in peak expression from the anaerobic to anoxic zone may have occurred due to limited anaerobic contact time to sufficiently induce expression of key carbon storage and energy metabolism genes. Redox conditions in the anaerobic zone are thought to be a significant contributing factor for successful EBPR. Achieving sufficiently low redox potential in the anaerobic zone can be limited due to high mixing energy that traps oxygen, low anaerobic zone SRTs, and introduction of flows with elevated dissolved oxygen (DO), such as from primary effluent during wet weather events.[46] Changes in influent VFA composition may have also contributed. many of the genes whose expression shifted were upregulated under high acetate conditions in lab-scale experiments suggesting changes in carbon availability may alter expression patterns.[35] If anaerobic-zone carbon availability is insufficient or oxidized, genes that normally peak in the anaerobic zone will peak in the anoxic zone, coincident with EBPR deterioration. Influent VFA concentration and oxidation-reduction potential (ORP) measurements across redox zones are necessary to definitively determine if either of the proposed hypotheses regarding anaerobic disruption are correct. Future studies should evaluate influent VFA concentration and composition

View Article Online
DOI: 10.1039/D5EW01105A

and profile basins for ORP, DO, and nitrate in parallel to microbial community and gene expression analyses.

Conclusions

This study evaluated a full-scale EBPR instability event using genome-centric metatranscriptomics and concluded that the instability was associated with changes in the activity rather than the composition of PAOs. The shift in peak expression of key carbon metabolism, denitrification, and energy production genes from the anaerobic zone to the anoxic zone strongly suggests that redox conditions and/or VFA availability in the anaerobic zone was compromised. Future studies of full-scale EBPR systems should couple metatranscriptomics with additional measurements, such as ORP, DO, and VFAs, to further develop the linkages necessary to understand underlying causes of instability events.

Code and Data Availability.

Raw sequencing data and high-quality MAGs are available in NCBI under BioProject PRJNA1232215. Medium quality MAGs are available upon request. Code used for data analyses is available in the following GitHub Repositories: https://github.com/jadeaver/bioP_MAGs (metagenomics code) and https://github.com/jadeaver/bioP_MT (metatranscriptomics code).

Acknowledgements

This work was supported by the STEPS Center, a US National Science Foundation Science and Technology Center (CBET-2019435). The authors are appreciative of

View Article Online
DOI: 10.1039/D5EW01105A

discussions and collaborations with various team members of the Science and Technologies for Phosphorus Sustainability (STEPS) Science and Technology Center. We also acknowledge the computing resources provided by North Carolina State University High Performance Computing Services Core Facility (RRID:SCR_022168). We thank our WRRF partner for providing samples, process data, and their knowledge and expertise during this study.

References

1. Merck AW, Deaver JA, Crane L, et al. Stakeholder Views of Science and Technologies for Phosphorus Sustainability: A Comparative Analysis. *Soc Nat Resour*. Published online August 13, 2024. doi:10.1080/08941920.2024.2389806

2. He S, Gu AZ, McMahon KD. Progress Toward Understanding the Distribution of *Accumulibacter* Among Full-Scale Enhanced Biological Phosphorus Removal Systems. *Microb Ecol*. 2008;55(2):229-236. doi:10.1007/s00248-007-9270-x

3. Neethling JB, Bakke B, Benisch M, et al. Factors Influencing the Reliability of Enhanced Biological Phosphorus Removal. Water Environment Research Foundation; 2005.

4. Wang D, Tooker NB, Srinivasan V, et al. Side-stream enhanced biological phosphorus removal (S2EBPR) process improves system performance - A full-scale comparative study. *Water Res*. 2019;167. doi:10.1016/j.watres.2019.115109

5. Dueholm MKD, Nierychlo M, Andersen KS, et al. MiDAS 4: A global catalogue of full-length 16S rRNA gene sequences and taxonomy for studies of bacterial communities in wastewater treatment plants. *Nat Commun*. 2022;13(1908). doi:10.1038/s41467-022-29438-7

6. McDaniel EA, Moya-Flores F, Beach NK, et al. Metabolic Differentiation of Co-occurring Accumulibacter Clades Revealed through Genome-Resolved Metatranscriptomics. *mSystems*. 2021;6(e00474-21). doi:10.1128/mSystems.00474-21

7. Guedes Da Silva L, Olavarria Gamez K, Castro Gomes J, et al. Revealing the Metabolic Flexibility of "*Candidatus Accumulibacter phosphatis*" through Redox Cofactor Analysis and Metabolic Network Modeling. *Appl. Environ. Microbiol*. 2020;86(24):e00808-20. doi:10.1128/AEM.00808-20

View Article Online
DOI: 10.1039/D5EW01105A

8. Law Y, Kirkegaard RH, Cokro AA, et al. Integrative microbial community analysis reveals full-scale enhanced biological phosphorus removal under tropical conditions. *Sci Rep*. 2016;6(1):25719. doi:10.1038/srep25719

9. Pérez MV, Guerrero LD, Orellana E, Figuerola EL, Erijman L. Time Series Genome-Centric Analysis Unveils Bacterial Response to Operational Disturbance in Activated Sludge. *mSystems*. 2019;4(4):e00169-19. doi:10.1128/mSystems.00169-19

10. Lindner B, Layton B, Lindner B, et al. Genome-centric Insights into Full-scale EBPR Captured During a Biomonitoring Campaign. In: *Proceedings of the Water Environment Federation*. Water Environment Federation; 2023. doi:10.2175/193864718825159085

11. Albertsen M, Karst SM, Ziegler AS, Kirkegaard RH, Nielsen PH. Back to Basics – The Influence of DNA Extraction and Primer Choice on Phylogenetic Analysis of Activated Sludge Communities. *PLOS ONE*. 2015;10(7):e0132783. doi:10.1371/journal.pone.0132783

12. Andrews S. FastQC: a quality control tool for high throughput sequence data. Babraham Bioinformatics. 2010. http://www.bioinformatics.babraham.ac.uk/projects/fastqc

13. De Coster W, Rademakers R. NanoPack2: population-scale evaluation of long-read sequencing data. *Bioinformatics*. 2023;39(5):btad311. doi:10.1093/bioinformatics/btad311

14. Holley G, Beyter D, Ingimundardottir H, et al. Ratatosk: hybrid error correction of long reads enables accurate variant calling and assembly. *Genome Biol*. 2021;22(28). doi:10.1186/s13059-020-02244-4

15. Kolmogorov M, Bickhart DM, Behsaz B, et al. metaFlye: scalable long-read metagenome assembly using repeat graphs. *Nat Methods*. 2020;17(11):1103-1110. doi:10.1038/s41592-020-00971-x

16. Wu YW, Simmons BA, Singer SW. MaxBin 2.0: an automated binning algorithm to recover genomes from multiple metagenomic datasets. *Bioinformatics*. 2016;32(4):605-607. doi:10.1093/bioinformatics/btv638

17. Kang DD, Li F, Kirton E, et al. MetaBAT 2: an adaptive binning algorithm for robust and efficient genome reconstruction from metagenome assemblies. *PeerJ*. 2019;7(e7359). doi:10.7717/peerj.7359

18. Sieber CMK, Probst AJ, Sharrar A, et al. Recovery of genomes from metagenomes via a dereplication, aggregation and scoring strategy. *Nat Microbiol*. 2018;3(7):836-843. doi:10.1038/s41564-018-0171-1

View Article Online
DOI: 10.1039/D5EW01105A

19. Olm MR, Brown CT, Brooks B, Banfield JF. dRep: a tool for fast and accurate genomic comparisons that enables improved genome recovery from metagenomes through de-replication. *ISME J*. 2017;11(12):2864-2868. doi:10.1038/ismej.2017.126

20. Schwengers O, Jelonek L, Dieckmann MA, Beyvers S, Blom J, Goesmann A. Bakta: rapid and standardized annotation of bacterial genomes via alignment-free sequence identification. *Microb Genomics*. 2021;7(000685). doi:10.1099/mgen.0.000685

21. Parks DH, Imelfort M, Skennerton CT, Hugenholtz P, Tyson GW. CheckM: Assessing the quality of microbial genomes recovered from isolates, single cells, and metagenomes. *Genome Res*. 2015;25(7):1043-1055. doi:10.1101/gr.186072.114

22. Chaumeil PA, Mussig AJ, Hugenholtz P, Parks DH. GTDB-Tk v2: memory friendly classification with the genome taxonomy database. Borgwardt K, ed. *Bioinformatics*. 2022;38(23):5315-5316. doi:10.1093/bioinformatics/btac672

23. Petriglieri F, Singleton CM, Kondrotaite Z, et al. Reevaluation of the Phylogenetic Diversity and Global Distribution of the Genus "*Candidatus Accumulibacter*." *mSystems*. 2022;7(3):e00016-22. doi:10.1128/msystems.00016-22

24. Lee MD. GToTree: a user-friendly workflow for phylogenomics. *Bioinformatics*. 2019;35(20):4162-4164. doi:10.1093/bioinformatics/btz188

25. Jain C, Rodriguez-R LM, Phillippy AM, Konstantinidis KT, Aluru S. High throughput ANI analysis of 90K prokaryotic genomes reveals clear species boundaries. *Nat Commun*. 2018;9(1):5114. doi:10.1038/s41467-018-07641-9

26. Woodcroft BJ, Aroney STN, Zhao R, et al. Comprehensive taxonomic identification of microbial species in metagenomic data using SingleM and Sandpiper. *Nat Biotechnol*. Published online June 12, 2025. doi:10.1038/s41587-025-02738-1

27. Oksanen J, Blanchet FG, Friendly M, et al. vegan: Community Ecology Package. Published online 2019. https://cran.r-project.org/package=vegan

28. Chen S, Zhou Y, Chen Y, Gu J. fastp: an ultra-fast all-in-one FASTQ preprocessor. *Bioinformatics*. 2018;34(17):i884-i890. doi:10.1093/bioinformatics/bty560

29. Kopylova E, Noé L, Touzet H. SortMeRNA: fast and accurate filtering of ribosomal RNAs in metatranscriptomic data. *Bioinformatics*. 2012;28(24):3211-3217. doi:10.1093/bioinformatics/bts611

30. Bray NL, Pimentel H, Melsted P, Pachter L. Near-optimal probabilistic RNA-seq quantification. *Nat Biotechnol*. 2016;34(5):525-527. doi:10.1038/nbt.3519

View Article Online
DOI: 10.1039/D5EW01105A

31. Love MI, Huber W, Anders S. Moderated estimation of fold change and dispersion for RNA-seq data with DESeq2. *Genome Biol*. 2014;15(550). doi:10.1186/s13059-014-0550-8

32. Bowers RM, Kyrpides NC, Stepanauskas R, et al. Minimum information about a single amplified genome (MISAG) and a metagenome-assembled genome (MIMAG) of bacteria and archaea. *Nat Biotechnol*. 2017;35(8):725-731. doi:10.1038/nbt.3893

33. Stewart RD, Myers KS, Amstadt C, Seib M, McMahon KD, Noguera DR. Refinement of the "*Candidatus Accumulibacter*" genus based on metagenomic analysis of biological nutrient removal (BNR) pilot-scale plants operated with reduced aeration. *mSystems*. 2024;9(3):e01188-23. doi:10.1128/msystems.01188-23

34. Petriglieri F, Singleton C, Peces M, Petersen JF, Nierychlo M, Nielsen PH. "*Candidatus Dechloromonas phosphoritropha*" and "*Ca. D. phosphorivorans*", novel polyphosphate accumulating organisms abundant in wastewater treatment systems. *ISME J*. 2021;15(12):3605-3614. doi:10.1038/s41396-021-01029-2

35. Oyserman BO, Noguera DR, Del Rio TG, Tringe SG, McMahon KD. Metatranscriptomic insights on gene expression and regulatory controls in *Candidatus Accumulibacter phosphatis*. *ISME J*. 2016;10(4):810-822. doi:10.1038/ismej.2015.155

36. He S, McMahon KD. *Candidatus Accumulibacter* gene expression in response to dynamic EBPR conditions. *ISME J*. 2011;5(2):329-340. doi:10.1038/ismej.2010.127

37. Qiu G, Liu X, Saw NMMT, et al. Metabolic Traits of *Candidatus Accumulibacter* clade IIF Strain SCELSE-1 Using Amino Acids As Carbon Sources for Enhanced Biological Phosphorus Removal. *Environ Sci Technol*. 2020;54(4):2448-2458. doi:10.1021/acs.est.9b02901

38. Chen L, Wei G, Zhang Y, et al. C*andidatus Accumulibacter* use fermentation products for enhanced biological phosphorus removal. *Water Res*. 2023;246:120713. doi:10.1016/j.watres.2023.120713

39. McDaniel EA, Van Steenbrugge JJM, Noguera DR, et al. TbasCO: trait-based comparative 'omics identifies ecosystem-level and niche-differentiating adaptations of an engineered microbiome. *ISME Commun*. 2022;2(1). doi:10.1038/s43705-022-00189-2

40. Camejo PY, Oyserman BO, McMahon KD, Noguera DR. Integrated Omic Analyses Provide Evidence that a "*Candidatus Accumulibacter phosphatis*" Strain Performs Denitrification under Microaerobic Conditions. Dutton RJ, ed. *mSystems*. 2019;4(1):e00193-18. doi:10.1128/mSystems.00193-18

41. Chen J, Strous M. Denitrification and aerobic respiration, hybrid electron transport chains and co-evolution. *Biochim Biophys Acta BBA - Bioenerg*. 2013;1827(2):136-144. doi:10.1016/j.bbabio.2012.10.002

View Article Online
DOI: 10.1039/D5EW01105A

42. Zharova TV, Grivennikova VG, Borisov VB. F1·Fo ATP Synthase/ATPase: Contemporary View on Unidirectional Catalysis. *Int J Mol Sci*. 2023;24. doi:10.3390/ijms24065417

43. Saunders AM, Mabbett AN, McEwan AG, Blackall LL. Proton motive force generation from stored polymers for the uptake of acetate under anaerobic conditions. *FEMS Microbiol. Lett*. 2007;274(2):245-251. doi:10.1111/j.1574-6968.2007.00839.x

44. Flowers JJ, He S, Yilmaz S, Noguera DR, McMahon KD. Denitrification capabilities of two biological phosphorus removal sludges dominated by different '*Candidatus Accumulibacter*' clades. *Environ Microbiol Rep*. 2009;1(6):583-588. doi:10.1111/j.1758-2229.2009.00090.x

45. Pitcher RS, Watmough NJ. The bacterial cytochrome cbb3 oxidases. *Biochim. Biophys. Acta*. 2004;1655:388-399. doi:10.1016/j.bbabio.2003.09.017

46. Barnard JL, Dunlap P, Steichen M. Rethinking the Mechanisms of Biological Phosphorus Removal. *Water Environ. Res*. 2017;89(11):2043-2054. doi:10.2175/106143017X15051465919010

47. Yun Z, Yun GH, Lee HS, Yoo TU. The variation of volatile fatty acid compositions in sewer length, and its effect on the process design of biological nutrient removal. *Water Sci. Technol*. 2013;67(12):2753-2760. doi:10.2166/wst.2013.192

View Article Online
DOI: 10.1039/D5EW01105A

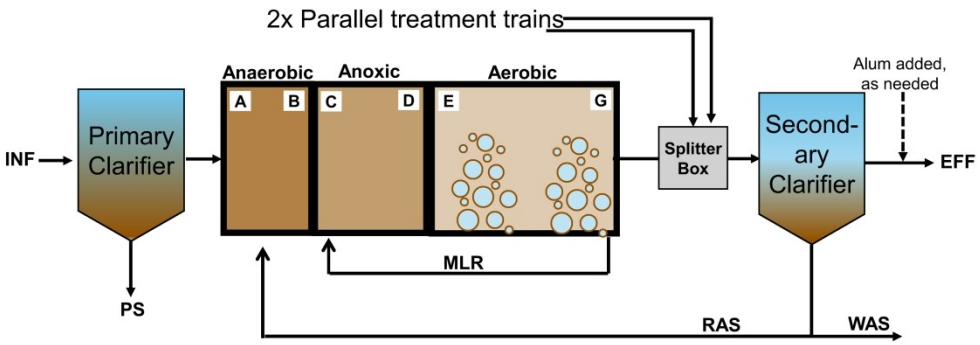

Figure 1

279x215mm (300 x 300 DPI)

View Article Online
DOI: 10.1039/D5EW01105A

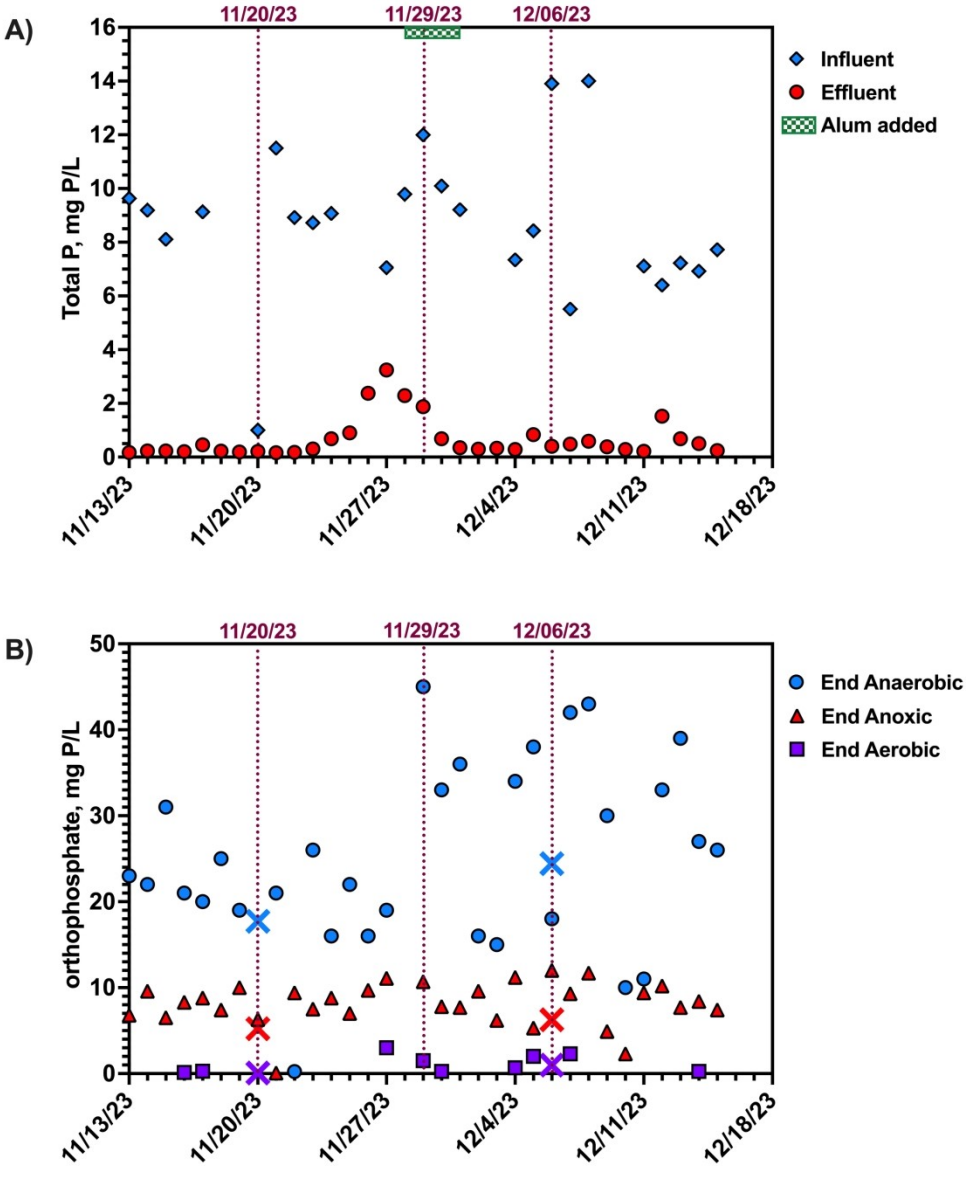

Figure 2

198x241mm (300 x 300 DPI)

View Article Online
DOI: 10.1039/D5EW01105A

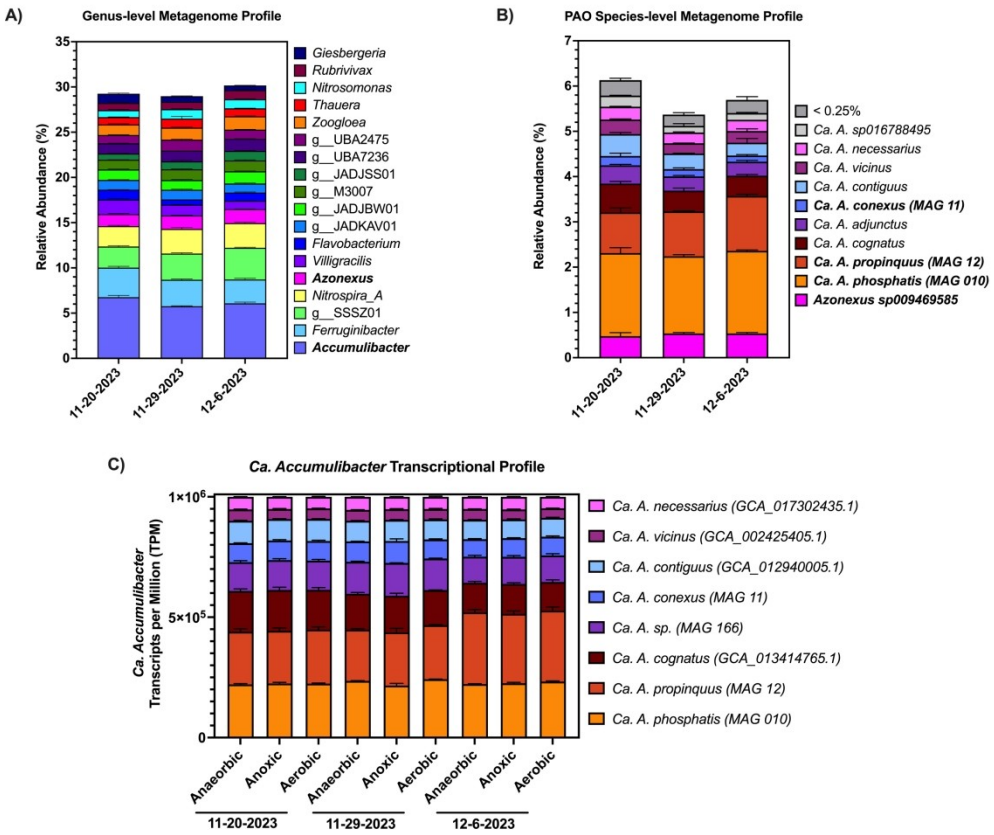

Figure 3

247x209mm (300 x 300 DPI)

View Article Online
DOI: 10.1039/D5EW01105A

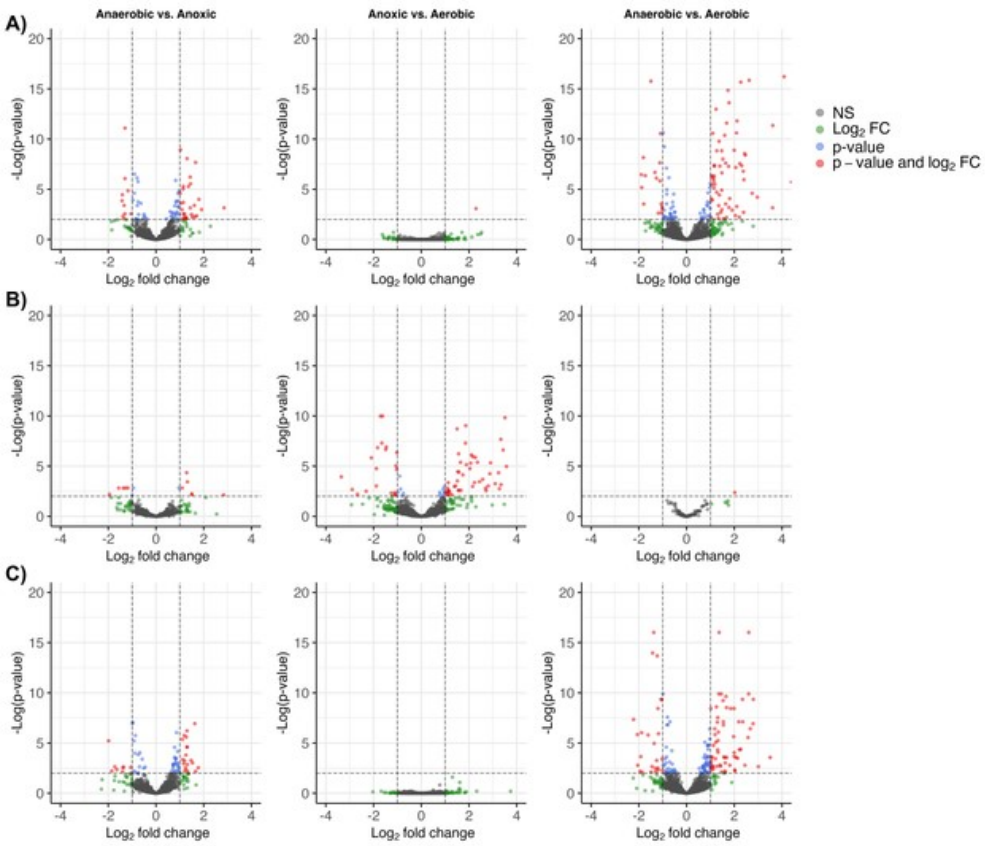

Figure 4

53x45mm (300 x 300 DPI)

View Article Online
DOI: 10.1039/D5EW01105A

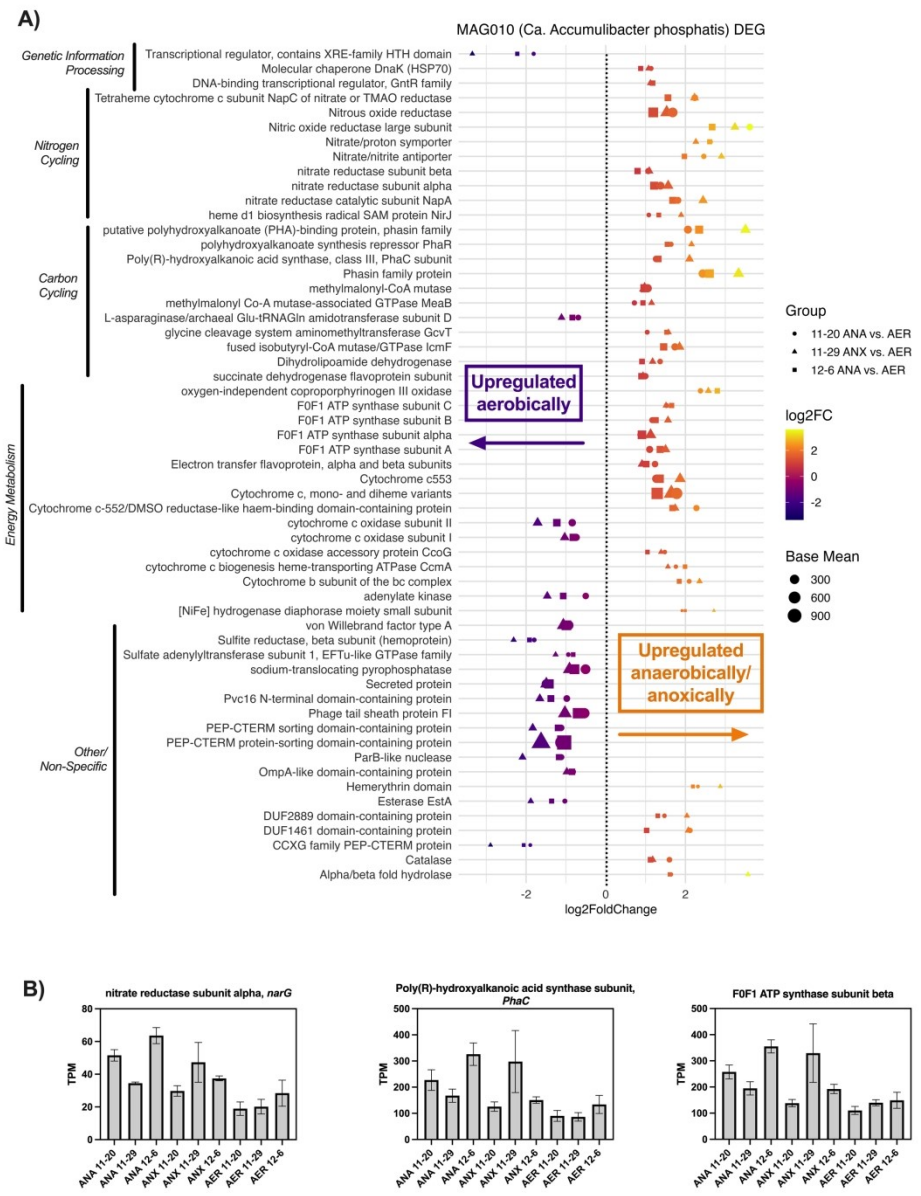

Figure 5

211x271mm (300 x 300 DPI)

View Article Online
DOI: 10.1039/D5EW01105A

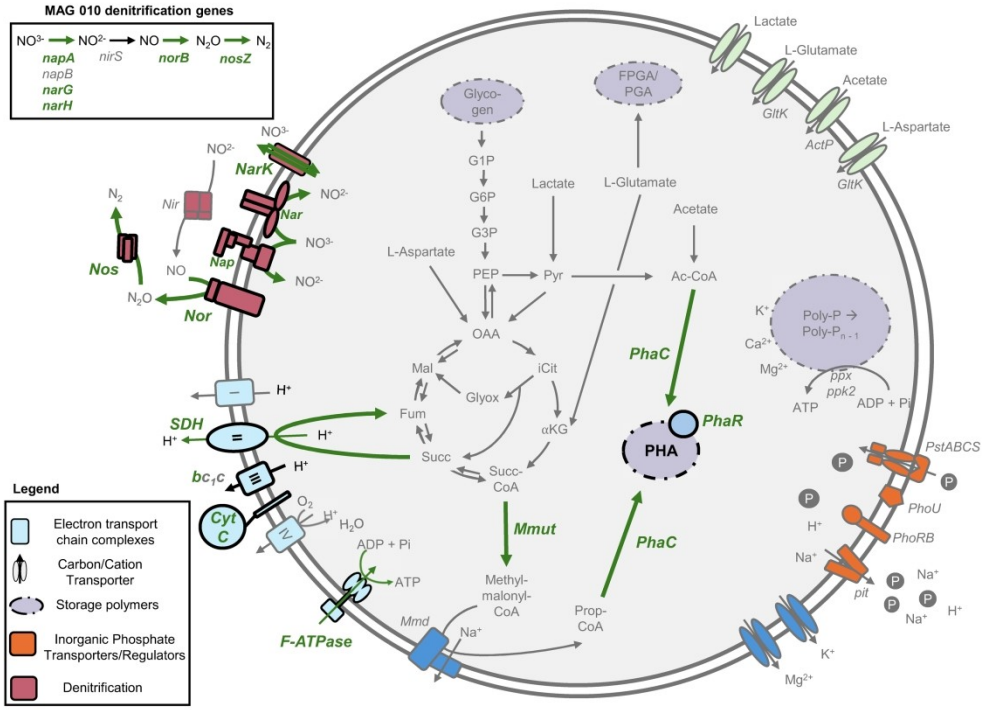

Figure

279x215mm (300 x 300 DPI)

View Article Online
DOI: 10.1039/D5EW01105A

Code and Data Availability.

Raw sequencing data and high-quality MAGs are available in NCBI under BioProject PRJNA1232215. Medium quality MAGs are available upon request. Code used for data analyses is available in the following GitHub Repositories: https://github.com/jadeaver/bioP_MAGs (metagenomics code) and https://github.com/jadeaver/bioP_MT (metatranscriptomics code).